

Isotopic fractionation of water during evaporation

Christopher D. Cappa,¹ Melissa B. Hendricks,^{1,2,3} Donald J. DePaolo,^{2,4} and Ronald C. Cohen^{1,4}

Received 14 March 2003; revised 9 June 2003; accepted 19 June 2003; published 30 August 2003.

[1] Variations in the isotopic content ($^{18}\text{O}/^{16}\text{O}$ and D/H ratios) of water in the natural environment provide a valuable tracer of the present-day global hydrologic cycle and a record of the climate over at least 400,000 years that is preserved in glacial ice. The interpretation of observed isotopic ratios in water vapor, rain, snow, and ice depends on our understanding of the processes (mainly phase changes) that produce isotopic fractionation. Whereas equilibrium isotopic fractionation is well understood, kinetic effects, or diffusion-controlled fractionation, has a limited experimental foundation. Kinetic effects are significant during evaporation into unsaturated air and during condensation to form ice from vapor. Kinetic effects are also thought to control the deuterium excess ($d = \delta\text{D} - 8\delta^{18}\text{O}$) of precipitation. We describe experiments to observe kinetic effects associated with evaporation. Analysis of our own and previous experiments shows that surface cooling of the liquid is a crucial variable affecting fractionation from evaporating water that has not been properly considered before. Including the effects of evaporative surface cooling reconciles observed D/H fractionation with kinetic theory and removes the need to invoke an unusual size for the HDO molecule. Thus the isotopic molecular diffusivity ratios are $D(\text{H}_2^{18}\text{O})/D(\text{H}_2^{16}\text{O}) = 0.9691$ and $D(\text{HD}^{16}\text{O})/D(\text{H}_2^{16}\text{O}) = 0.9839$. Implications of this work for representation of kinetic fractionation in global circulation models and cloud physics models are briefly discussed.

INDEX TERMS: 0320 Atmospheric Composition and Structure: Cloud physics and chemistry; 0322 Atmospheric Composition and Structure: Constituent sources and sinks; 1655 Global Change: Water cycles (1836); 1899 Hydrology: General or miscellaneous; *KEYWORDS:* evaporation, water isotopes, deuterium excess, hydrologic cycle

Citation: Cappa, C. D., M. B. Hendricks, D. J. DePaolo, and R. C. Cohen, Isotopic fractionation of water during evaporation, *J. Geophys. Res.*, 108(D16), 4525, doi:10.1029/2003JD003597, 2003.

1. Introduction

[2] Water plays a central role in atmospheric chemistry and climate. Despite the obvious importance of water we still lack a mechanistic understanding of its global cycle that permits rigorous scaling of molecular properties and processes to the kilometer scales of clouds and the global scales of moisture transport. The most detailed and important sources of data constraining climate change during the last 400,000 years are records of the isotopic ratios of $^{18}\text{O}/^{16}\text{O}$ and D/H from glacial ice in Antarctica [Petit et al., 1999; Vimeux et al., 2001] and Greenland [White et al., 1997]. However, the processes that affect isotopic ratios in high-latitude precipitation are complex, making direct inference

of paleotemperatures and other climate parameters from the isotopic record difficult [e.g., Cuffey et al., 1994; Jouzel et al., 1997; Hendricks et al., 2000].

[3] Evaporation, as the first step in the hydrologic cycle, plays a crucial role in determining isotope ratios found in global precipitation and ice core records. In addition, isotope effects during evaporation from plants determine the isotopic composition of oxygen in atmospheric CO_2 and O_2 [Farquhar et al., 1993; Bender et al., 1994]. If the atmosphere-ocean system was in thermodynamic equilibrium, then determination of the isotope ratios in evaporation would be a trivial problem, as equilibrium vapor pressure isotope effects are well understood both theoretically [Bigeleisen, 1961] and experimentally [Horita and Wesolowski, 1994]. The atmosphere is, however, an inherently nonequilibrium system, and both microscopic properties of water and macroscopic transport of water molecules through the air are important controls over isotope fractionation in water vapor and in precipitation [Craig and Gordon, 1965; Merlivat and Jouzel, 1979; Hendricks et al., 2000; Kavanaugh and Cuffey, 2003]. In the language of atmospheric modelers the transport effects are referred to as kinetic effects, not to be confused with a standard kinetic isotope effect, which refers to isotope-

¹Department of Chemistry, University of California, Berkeley, Berkeley, California, USA.

²Berkeley Center for Isotope Geochemistry, Earth Sciences Division, Lawrence Berkeley National Laboratory, Berkeley, California, USA.

³Now at Department of Geosciences, Princeton University, Princeton, New Jersey, USA.

⁴Department of Earth and Planetary Science, University of California, Berkeley, Berkeley, California, USA.

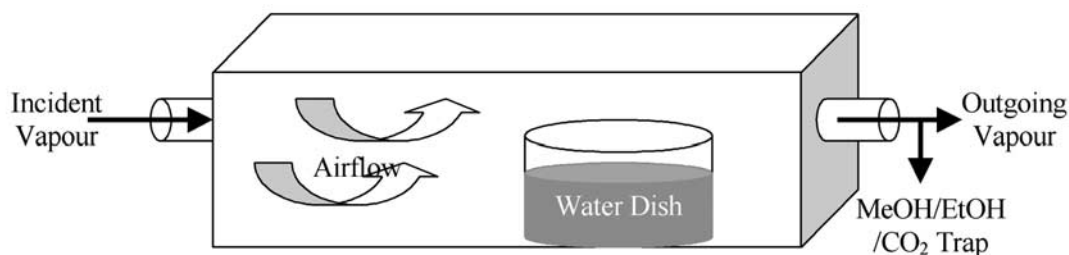


Figure 1. Experimental setup.

dependent reaction rates of a specific microscopic process. *Craig et al.* [1963] showed that kinetic effects and molecular exchange between an evaporating liquid and atmospheric water vapor both affect fractionation during evaporation. Experiments by *Stewart* [1975] and *Merlivat and Coantic* [1975] confirmed that these kinetic effects are present during evaporation from liquid droplets and that the total fractionation depends on relative humidity of the ambient environment.

[4] The theoretical formulation of kinetic effects during evaporation as implemented in most global circulation models (GCMs) is based on the work of *Merlivat and Jouzel* [1979]. Underlying this model is a physical description of evaporation that accounts for transport of water isotopomers between the liquid-air interface and the turbulent boundary layer and that depends explicitly on both the relative humidity and water surface temperature. The microphysical predictions from this model have not been rigorously tested, although they are loosely consistent with laboratory data. Comparison of global scale predictions from GCMs fitted with water isotope transport schemes using this parameterization have been extensively compared with atmospheric precipitation measurements of δD and $\delta^{18}O$ obtained by the IAEA and others [*Jouzel et al.*, 1987; *Armengaud et al.*, 1998; *Hoffmann et al.*, 1998; *Jouzel et al.*, 2000]. (The δ notation is defined as $\delta^{18}O$ (or δD) = $1000(R_{\text{sample}}/R_{\text{SMOW}} - 1)$, where $R \equiv [^{18}O]/[^{16}O]$ (or $R \equiv [D]/[H]$) and R_{SMOW} is the corresponding ratio in Vienna standard mean ocean water (SMOW) or V-SMOW.) The δD and $\delta^{18}O$ model output from GCMs yields a reasonable approximation to measurements. However, a large discrepancy in the deuterium excess ($d = \delta D - 8\delta^{18}O$ [*Dansgaard*, 1964]) is found. This is particularly clear at high latitudes where differences of 2–5‰ have been reported between model and observation [*Hoffmann et al.*, 1998; *Jouzel et al.*, 2000] and in simulations of seasonal distributions of d , which produce cycles that are much larger than that observed and even give unrealistic negative values [*Jouzel et al.*, 1987; *Werner et al.*, 1998].

[5] Equilibrium considerations yield a value of d close to zero at 25°C, whereas the value of d in global precipitation is found to be near +10‰. The sensitivity of d to temperature under equilibrium conditions is $0.4\text{‰ } ^\circ\text{C}^{-1}$, which implies that a value of $d = +10\text{‰}$ corresponds to an equilibrium temperature of 70°C; one clear indication that an equilibrium approximation is a poor representation of isotopes in the Earth's hydrologic cycle. This positive difference is usually explained as resulting from diffusive transport playing a large role in evaporation. Diffusive transport leads to greater fractionation of the light iso-

topomers during nonequilibrium processes when molecular diffusion (as opposed to turbulent diffusion) is important. Thus the deuterium excess in precipitation and atmospheric water vapor provides information about the role of diffusive transport in the boundary layer at the evaporative source and about source temperatures that cannot be obtained from δD or $\delta^{18}O$ individually. The particular difficulties associated with modeling d in GCMs and other less-complex models indicate that there may be a problem associated with how evaporation is parameterized in these models.

[6] In this paper we describe new experiments to measure the fractionation of water during evaporation. Our analysis focuses on the diffusivity ratios of $H_2^{18}O/H_2^{16}O$ and HDO/H_2O in N_2 , and we reconsider models of evaporation in light of the recent experiments by *Ward and Stanga* [2001], who measured significant surface cooling in the top few millimeters of evaporating water.

2. Methods

[7] We measured isotopic ratios of both liquid and vapor samples during evaporation of the liquid into an airstream of constant relative humidity (h). The constant h airstream was generated by mixing dry and saturated airstreams in the appropriate ratio. The saturated airstream was generated by flowing dry N_2 derived from the boil off of liquid N_2 through a series of six 4-L bubblers filled with distilled water. The final bubbler was temperature regulated in order to control the absolute amount of water vapor present in the airstream. The flow rates of the dry (F_{dry}) and saturated (F_{sat}) N_2 streams were independently controlled using mass-flow controllers (MKS type 1179A). The two nitrogen streams were recombined ($F = F_{\text{dry}} + F_{\text{sat}}$) and directed into a sealed, temperature-regulated chamber ($l \times w \times h = 0.38 \text{ m} \times 0.13 \text{ m} \times 0.07 \text{ m}$), see Figure 1. The relative humidity and temperature were continuously monitored in the inflow to the chamber, within the chamber just above the evaporation dish and in the outflow from the chamber using a set of hygrometers (HIH-3602C) and thermocouples (Omega 5TC-TT-K-36-72). A small fan was used inside the chamber to enhance mixing. The outflow could be directed through a water vapor trap for vapor collection. The trap consisted of Teflon tubing (1.27 cm i.d.) in four loops placed in a MeOH/EtOH/dry ice bath such that the total length of tubing in the alcohol bath was $\sim 1.22 \text{ m}$.

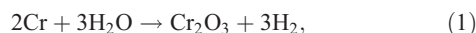
[8] Distilled water was used for all experiments without further purification or degassing. At the start of each experiment a sample of the incident vapor was collected. A glass dish ($r = 3.28 \text{ cm}$, $h = 5.07 \text{ cm}$) was filled with

Table 1. Experimental Conditions and Evaporation Rates

h_{in} , %	Trial	h_{out} , %	T_{in} , °C	T_{out} , °C	F , mmol s ⁻¹	T_{liq} , °C	Measured E , mmol m ⁻² s ⁻¹	Calculated E , mmol m ⁻² s ⁻¹
51.2	a	60.8	19.4	18.9	6.96	18.8	3.65	3.65
51.4	b	66.5	20.0	20.0	3.45	19.9	3.52	3.56
20.4		45.3	20.0	20.1	6.96	19.8	5.94	6.03
0	a	10.3	20.0	20.4	6.96	19.9	7.08	5.02
0	b	18.9	19.6	19.3	6.96	18.8	8.45	8.58

water precooled to the same temperature as the final bubbler. An initial water sample was collected, the start mass recorded, and the water dish placed in the chamber. The chamber was sealed, and a sample of the outgoing vapor was collected. At the end of each measurement period, typically 24 hours, the same three water samples were collected (the vapor out, liquid, and vapor in). The water dish was weighed before and after the liquid sample was taken.

[9] Isotope analyses of the samples were carried out on a Finnegan-MAT Delta Plus XL isotope ratio mass spectrometer at the Center for Stable Isotope Biogeochemistry at the University of California at Berkeley. Water ¹⁸O/¹⁶O ratios were determined by the standard CO₂ equilibration technique [Bottinga and Craig, 1969]. Water D/H ratios were determined by reduction of the water samples to H₂ (H₂O) and HD (HDO) over a chromium catalyst maintained at 900°C



with subsequent measurement of the hydrogen isotope ratios [Donnelly et al., 2001]. Isotopic ratios were determined relative to internal standards, and delta values are expressed relative to V-SMOW ($\delta = R/R_{V-SMOW} - 1$).

[10] Separate experiments at different humidities and gas flow rates were conducted. The average evaporation rate, E , was calculated for each experiment from the measured decrease in liquid mass over time. The evaporation rate decreased slightly over the course of each experiment as the liquid level dropped in the evaporation dish. This measured value can be compared to the evaporation rate calculated from mass balance, which requires [von Caemmerer and Farquhar, 1981]

$$E = F \frac{(w_0 - w_e)}{(1 - w_0)}, \quad (2)$$

where F is the total flow rate in moles per second and w_x is the mole fraction of water entering ($x = e$) and exiting ($x = 0$) the chamber. The mole fractions are determined from the partial pressure of water, p , relative to the pressure at the outlet (ambient). The water vapor partial pressures are calculated from the measured relative humidity and temperature, where $p = hp^0$ with p^0 the saturation vapor pressure at that temperature as given by Wexler [1976]. Table 1 lists the conditions of each experiment as well as the measured and calculated evaporation rates. For all experiments the calculated evaporation rate is the same as the measured value, with the exception of one of the 0% h runs (run a), which indicated that the partial pressure of water in the outgoing

vapor for this experiment as determined from h_{out} and T_{out} is too small. If the error is in the h measurement rather than the temperature measurement, then the relative humidity of the outgoing vapor was 14.5%, instead of the 10.3% observed. It is unclear what caused this error as the discrepancy is outside the specified accuracy ($\pm 2\%$) of the hygrometer.

3. Results and Discussion

[11] The ¹⁸O/¹⁶O and D/H isotope ratios measured during each stage in the liquid and outgoing vapor are listed in Table 2. For all experiments the liquid (and consequently the outgoing vapor) became isotopically heavier as evapo-

Table 2. Isotope Ratios Measured in the Liquid and Outgoing Vapor for Each Experiment^a

Stage	f_{tot} Total	f Stage	Liquid		Vapor Out		α_{eff}^*	
			$\delta^{18}O$	δD	$\delta^{18}O$	δD	¹⁸ O/ ¹⁶ O	D/H
50% h (Trial a)								
0	1		-13.08	-95.36	-24.29	-167.48		
1	0.67	0.67	-7.24	-69.78	-22.31	-160.34	0.9851	0.9249
2	0.5	0.74	-4.31	-55.31	-22.03	-159.56	0.9901	0.9479
3	0.36	0.72	-2.02	-44.76	-21.71	-157.51	0.9929	0.9656
4	0.21	0.58	0.21	-32.77	-20.9	-153.54	0.9959	0.9771
5	0.15	0.71	1.02	-27.87	-20.34	-150.92	0.9977	0.9853
50% h (Trial b)								
0	1		-13.75	-95.81	-24.85	-166.87		
1	0.96	0.96	-12.97	-92.51	-24.73	-166.97	0.9817	0.9161
2	0.87	0.91	-11.65	-86.16	-23.53	-163.63	0.9854	0.9240
3	0.74	0.85	-9.26	-75.98	-22.61	-159	0.9851	0.9318
4	0.58	0.78	-6.57	-63.51	-21.45	-155	0.9892	0.9465
5	0.45	0.78	-4.48	-53.41	-20.26	-149.94	0.9917	0.9577
6	0.25	0.55	-1.71	-38.23	-18.97	-143.06	0.9954	0.9734
20% h								
0	1		-13.82	-95.95	-27.36	-168.51		
1	0.84	0.84	-10.96	-82.8	-25.44	-161.82	0.9830	0.9150
2	0.73	0.87	-8.6	-71.93	-23.88	-155.24	0.9836	0.9187
3	0.61	0.84	-5.96	-59.09	-21.62	-147.29	0.9848	0.9216
4	0.49	0.82	-2.82	-44.41	-19.06	-135.36	0.9844	0.9234
5	0.39	0.79	0.55	-27.79	-17.41	-128.01	0.9855	0.9260
0% h (Trial a)								
0	1		-13.2	-94.1	-32.73	-151.84		
1	0.69	0.69	-5.85	-64.81	-26.37	-147.09	0.9797	0.9131
2	0.44	0.63	3.67	-26.7	-17.16	-111.6	0.9791	0.9126
3	0.32	0.72	10.53	2.62	-10.44	-86.74	0.9790	0.9086
4	0.15	0.47	27.48	75.23	4.79	-23.16	0.9780	0.9074
0% h (Trial b)								
0	1		-13.42	-93.99	-31.86	-169.49		
1	0.75	0.75	-7.67	-70.02	-26.81	-150.78	0.9800	0.9102
2	0.39	0.52	4.74	-16.45	-14.35	-102.41	0.9810	0.9142
3	0.11	0.29	29.01	99.92	8.95	-0.71	0.9806	0.9091

^aValues are given in ‰.

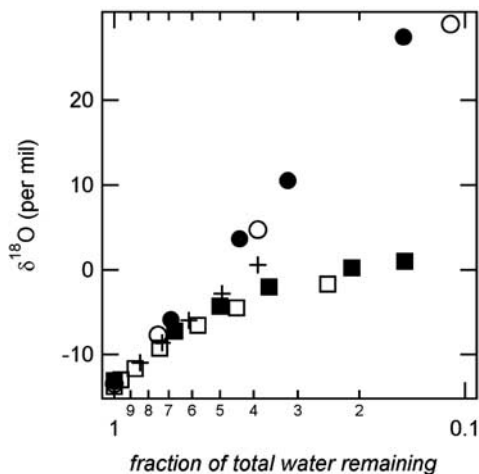


Figure 2. Evolution of $\delta^{18}\text{O}$ over the course of each experiment is shown versus f_{tot} (on a logarithmic scale). A linear relationship is observed for $h_{\text{in}} = 0\%$ (trial a, solid circle) and (trial b, open circle) and $h_{\text{in}} = 20\%$ (+), whereas for $h_{\text{in}} = 50\%$ (trial a, solid square) and (trial b, open square) the isotopic ratios approach steady state as $f \rightarrow 0$.

ration progressed. In an equilibrium batch distillation the isotopic ratio of the liquid should evolve according to the Rayleigh equation,

$$\ln(R_{\text{liq}}/R_{\text{liq},t=0}) = (\alpha_{\text{eff}}^* - 1) \ln f, \quad (3)$$

where R_{liq} is the isotopic ratio in the liquid at the end of each stage, $R_{\text{liq},t=0}$ is the ratio at the start of each stage, f is the fraction of water remaining at the end of each stage and α_{eff}^* is the effective fractionation factor during that stage (where the asterisk indicates that the fractionation factors are for the liquid/vapor). Although the system under consideration is not an equilibrium system, an average effective fractionation factor can be calculated for each stage of the experiments, with the assumption that the variation in the isotopic ratios over each time step is approximately linear, which is what was observed. In particular, during the experiments where $h_{\text{in}} = 0\%$ and $h_{\text{in}} = 20\%$, the effective fractionation factor was nearly constant over the course of the experiment because the variation in the isotopic composition of the liquid is linear against $\ln f_{\text{liq}}$ (Figure 2). However, for the experiments where $h_{\text{in}} > 20\%$, $\alpha_{\text{eff}}^* \rightarrow 1$ as $\ln f_{\text{liq}} \rightarrow 0$ because the isotopic ratios of the liquid and the evaporation approach a stationary value at long times. This is caused by the higher flux of water molecules transferred from the vapor to the liquid in the experiments when $h > 20\%$. Nonetheless, we have collected water and vapor samples sufficiently often that use of the Rayleigh equation for each stage is still valid for the experiments where α_{eff}^* is not a constant ($h_{\text{in}} > 20\%$).

[12] If we assume that the boundary layer between the liquid surface and the “free atmosphere” is at evaporative steady state, then the effective fractionation factor, α_{eff}^* in equation (3), can be expressed as

$$\alpha_{\text{eff}}^* = \alpha_{\text{diffusion}}^* \left[\frac{\alpha_{\text{eqm}}^* - h(R_a/R_l)}{1 - h} \right], \quad (4)$$

where α_{eqm}^* is the temperature-dependent equilibrium fractionation factor, h is the relative humidity, R_a is the isotopic ratio of the “free atmosphere,” R_l is the isotopic ratio in the liquid and $\alpha_{\text{diffusion}}^*$ is a fractionation term that accounts for differences in the molecular transport properties of the water isotopomers [Hendricks, 1999]. Equation (4) is derived in detail in Appendix A. For these experiments, $R_a = R_{\text{out}}$ and $h = h_{\text{out}}$. The equilibrium fractionation factors used in application of equation (4) were calculated using the bulk water temperature, and the expressions were reported by Horita and Wesolowski [1994] for both D/H and $^{18}\text{O}/^{16}\text{O}$ fractionation.

[13] All the terms in equation (4) are known except for $\alpha_{\text{diffusion}}^*$. We estimate $\alpha_{\text{diffusion}}^* = K_H/K_L$ where K is a turbulent diffusion constant that takes into account the effects of turbulence on the system and H indicates the heavy isotopomer and L the light isotopomer. As a simple first approximation this turbulent diffusivity ratio can be written as [Stewart, 1975]

$$\alpha_{\text{diffusion}}^* \frac{K_H}{K_L} = \left[\frac{D_H}{D_L} \right]^n, \quad (5)$$

where D is the molecular diffusivity and n is a parameter that ranges from 0 (completely turbulent diffusion) to 1 (molecular diffusion). For water vapor in N_2 at 0°C the molecular diffusivity is $2.190 \times 10^{-5} \text{ m}^2 \text{ s}^{-1}$ [Massman, 1998].

[14] The molecular diffusivity ratio can be calculated from the kinetic theory of gases as

$$\frac{D_H}{D_L} = \left(\frac{M_L(M_H + M_G)}{M_H(M_L + M_G)} \right)^{1/2} \left(\frac{\Gamma_L + \Gamma_G}{\Gamma_H + \Gamma_G} \right)^2, \quad (6)$$

where M is the molecular mass of the water isotopomer, and Γ is the collision diameter of the molecules. The subscript G refers to the bath gas. For isotopomeric molecules, we assume that the collision diameters are identical, and therefore D_H/D_L depends only on the masses. D_H/D_L is equal to 0.984 and 0.969 for $\text{HD}^{16}\text{O}/\text{H}_2^{16}\text{O}$ and $\text{H}_2^{18}\text{O}/\text{H}_2^{16}\text{O}$ diffusion in N_2 , respectively. This assumption conflicts with the analysis of Merlivat [1978], henceforth referred to as M78, that argues for different collision diameters and is discussed in more detail below.

[15] In Figure 3 we show the $\delta\text{D}-\delta^{18}\text{O}$ relationship observed for each experiment. The average slope for all experiments is 4.34, rather than the value of ~ 8 of the meteoric water line. Differences in turbulent diffusion are largely responsible for the range of d excess observed in the lab and on the Earth. Despite the different δ - f relationships observed for each experiment (depending on the particular experimental conditions), the same linear $\delta\text{D}-\delta^{18}\text{O}$ relationship is observed for all the experiments. The $\delta\text{D}-\delta^{18}\text{O}$ slope is approximately the same in the five different experiments because the diffusion effects are similar in these five experiments.

3.1. Surface Cooling

[16] If heat is not supplied rapidly to the surface of an evaporating liquid the endothermic nature of the process will cause the surface to cool below the bulk value. Recently, Ward and Stanga [2001] have shown that this

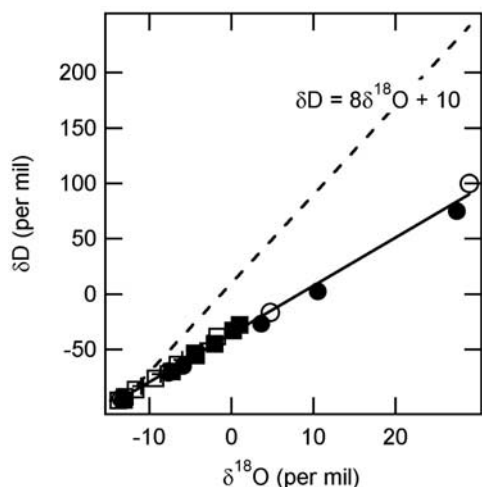


Figure 3. The δD versus $\delta^{18}O$ (liquid) values for each experiment. A linear relationship is observed with a best fit to all the data of $\delta D = 4.34\delta^{18}O - 35.8$. See Figure 2 for symbols.

cooling may be large ($>25^{\circ}C$) for H_2O when evaporation is fast and that the temperature gradient that is induced persists within only the top few millimeters of the liquid surface. Additionally, they observed an ~ 0.5 -mm-thick layer at the surface of evaporating H_2O that has an approximately uniform temperature that is colder than the bulk. On the basis of their measurements we assume that the surface of the evaporating water in our experiments is cooler than the bulk liquid temperature. As the molecules evaporate at the surface, the value of α_{eqm}^* used in equation (4) should be a larger number, one appropriate for a cooled surface rather than the value that corresponds to the bulk temperature. This change in α_{eqm}^* affects D/H fractionation to a larger extent than $^{18}O/^{16}O$ fractionation due to the stronger temperature dependence of α_{eqm}^* (D/H).

[17] Using data from Fang and Ward [1999] we calculate that the surface cooling at $\sim 19^{\circ}C$ and evaporation rates of $\sim 4.57 \text{ mmol m}^{-2} \text{ s}^{-1}$ should be $\sim 0.505^{\circ}C \text{ mmol}^{-1} \text{ m}^{-2} \text{ s}^{-1}$. For the surface area of our evaporation dish ($3.38 \times 10^{-3} \text{ m}^2$) this translates to surface cooling for the 50% h_{in} experiments of $1.9^{\circ}C$ (trial a) and $1.8^{\circ}C$ (trial b), for the 20% h_{in} experiment of $3.0^{\circ}C$ and for the 0% h_{in} experiments of $3.6^{\circ}C$ (trial a) and $4.3^{\circ}C$ (trial b).

[18] The influence of surface cooling on $\alpha_{diffusion}^*$ is shown in Figure 4 (note the difference in the x and y scales). We calculate $\alpha_{diffusion}^*$ for the 20% h experiment using coolings of 0° , 1° , 3° , and $5^{\circ}C$. For a surface cooling of $\sim 3^{\circ}C$, the measured values of $\alpha_{diffusion}^*$ are in accordance with $\alpha_{diffusion}^*$ calculated with equation (5), using a value of 0.40 for n and our assumption that all the H_2O isotopomers have the same collision diameter. This average value of n was determined from equation (6) and the experimentally derived $\alpha_{diffusion}^*$ for both D/H and $^{18}O/^{16}O$ fractionation. Without surface cooling our model would be incapable of representing the observations and we would be led to the same conclusion as M78 that different collision diameters are required to give the model the flexibility needed to describe the observations. We solve for $\alpha_{diffusion}^*$ for each experiment (Table 3). The reported values are the average of

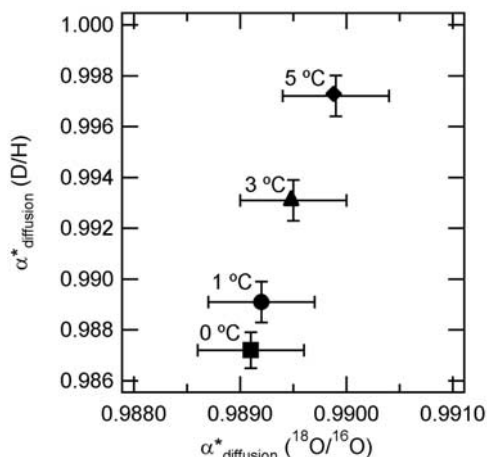


Figure 4. The $\alpha_{diffusion}^*$ values calculated for D/H and $^{18}O/^{16}O$ fractionation for the 20% h experiment using the bulk liquid temperature (solid square), and surface coolings of 1° (solid circle), 3° (solid triangle), and $5^{\circ}C$ (solid diamond). The reported values are the average of all stages for this experiment, and the error bars are the standard deviation of the average.

all stages for a given experiment and the 1σ values are the standard deviation of the average. We compare the surface coolings calculated from the observed evaporation rates to those required to bring the results from each experiment into exact agreement with the kinetic theory and our approximation of the form of $\alpha_{diffusion}^*$ (equation (6)). For this model, it is necessary that n is conserved between D/H and $^{18}O/^{16}O$ fractionation. Thus equation (6) can be rearranged to determine n for the experiment, and the surface cooling, which controls $\alpha_{diffusion}^*$, can be adjusted until $n(D/H) = n(^{18}O/^{16}O)$. The surface coolings required are 2.0° and $1.1^{\circ}C$ for 50% h_{in} (trial a) and (trial b), $4.0^{\circ}C$ for 20% h_{in} , and 6.4° and $5.0^{\circ}C$ for 0% h_{in} (trial a) and (trial b), corresponding to n values of 0.33, 0.32, 0.33, 0.39, and 0.37, respectively. The values are consistent, although not identical to the coolings listed in Table 3, which are calculated based on the measured evaporation rates. In contrast, if the M78 diffusivity ratios are used a physically unrealistic surface “warming” of a few tenths of a degree is required to explain the 50% (trial b) h_{in} results with $n = 0.37$, and the largest surface cooling is predicted for the

Table 3. Average Diffusion-Controlled Fractionation Factors, $\alpha_{diffusion}^*$, Determined for Each Experiment After Including the Effect of Surface Cooling^a

Experiment	D/H		$^{18}O/^{16}O$		$\Delta T, K$
	$\alpha_{diffusion}^*$	1σ	$\alpha_{diffusion}^*$	1σ	
50% (trial a)	0.9943	0.0021	0.9898	0.0003	-1.9
50% (trial b)	0.9969	0.0027	0.9901	0.0013	-1.8
20%	0.9926	0.0006	0.9895	0.0004	-3.0
0% (trial a)	0.9902	0.0038	0.9876	0.0007	-3.6
0% (trial b)	0.9925	0.0031	0.9885	0.0006	-4.3

^a ΔT is the amount of surface cooling expected based on the measured evaporation rate as calculated from the results of Fang and Ward [1999].

Table 4. D_i/D as Calculated From Equation (8) and Measured by Stewart [1975] for HD¹⁶O Versus H₂¹⁶O^a

	N ₂	Ar	He
	<i>Equation (8)</i>		
Single size parameter	0.984	0.982	0.995
Isotope-dependent size (M78)	0.976	0.973	0.985
	<i>Stewart [1975]</i>		
Surface cooling = 0°C	0.980	0.977	0.991
Surface cooling = 2°C	0.985	0.982	0.995

^aThe calculated values are considered with the collision diameters of the water isotopomers equal and with those determined by M78.

20% h_{in} results rather than for the dry N₂ experiments, as is expected from the observed evaporation rates.

3.2. Molecular Diffusivity Ratios

[19] Experiments observing δD and $\delta^{18}O$ of evaporation described in M78 were interpreted as demonstrating D_{HDO}/D_{H_2O} equal to 0.9755 and $D_{H_2^{18}O}/D_{H_2^{16}O}$ equal to 0.9727. These values are quite different from those predicted by the kinetic theory of gases (0.9839 for D/H and 0.9691 for ¹⁸O/¹⁶O). It was suggested in M78 that this difference was due to the various water isotopomers having different collision diameters. If surface cooling effects are considered rather than collision diameter differences for the M78 measurements, then a surface cooling of $\sim 4.1^\circ C$ explains the M78 measurements without invoking different collision diameters. This amount of cooling would be associated with an evaporation rate of $8.10 \text{ mmol m}^{-2} \text{ s}^{-1}$ or $3.24 \times 10^{-5} \text{ mol s}^{-1}$ ($A = 4 \times 10^{-3} \text{ m}^2$), not an unreasonable value. Unfortunately, the experimental evaporation rates are not reported by M78 for comparison.

[20] Although surface cooling does allow us to make sense of the D/H observations of M78, the ¹⁸O/¹⁶O results described in their paper cannot be explained by surface cooling. M78 suggests that the diffusivity ratio of ¹⁸O/¹⁶O is larger than that predicted from kinetic theory, and the data were interpreted to imply $\Gamma_{H_2^{16}O} > \Gamma_{H_2^{18}O}$ or $\Gamma_{H_2^{18}O} > \Gamma_{H_2^{16}O} = 0.995_5$. In addition to the evidence for surface cooling from Ward and Stanga [2001] and our own observations there is little evidence for isotopic size differences large enough to affect diffusivity ratios to the extent indicated by M78. The collision diameter of a molecule is determined primarily by the strength of interaction between molecules (Van der Waals forces, dispersion forces, etc.) and only secondarily by the actual molecular dimensions (bond lengths, angles). Therefore for isotopomeric molecules such as H₂¹⁶O, H₂¹⁸O, and HDO the collision diameters should be identical under the Born-Oppenheimer approximation [Hirschfelder, 1954]. We have found no satisfactory explanation for the ¹⁸O/¹⁶O measurements of M78 and suggest that additional effort to observe ¹⁸O/¹⁶O ratios in evaporation would be useful.

[21] Our surface cooling analysis is, however, consistent with all other experiments we are aware of that observe isotope effects during evaporation of H₂O. Experiments by Stewart [1975] indirectly measured D_H/D_L for water in N₂, Ar, and He. In Table 4 we calculate D_H/D_L for HD¹⁶O/H₂¹⁶O in N₂, Ar, and He from equation (8) and using the data from Stewart [1975]. If a surface cooling of 2°C is assumed for the water droplets in the Stewart experiments

the D/H results are in nearly exact agreement with the kinetic theory when $\Gamma_H = \Gamma_L$. If the collision diameter ratios from M78 are used in equation (8), the calculated values of D_H/D_L are too small for D/H and too large for ¹⁸O/¹⁶O to be consistent with Stewart's measurements. The collision diameters used were $\Gamma(N_2) = 3.7 \text{ \AA}$, $\Gamma(Ar) = 3.58 \text{ \AA}$, $\Gamma(He) = 2.15 \text{ \AA}$, and $\Gamma(H_2^{16}O) = 4.42 \text{ \AA}$ [Lide, 2001]. There is also better agreement of the ratios for ¹⁸O/¹⁶O, but the differences are more subtle due to the weak temperature dependence of α_{eqm}^* (¹⁸O/¹⁶O).

[22] As additional evidence for identical collision diameters for isotopomers, consider N₂ and CO, which are isoelectronic molecules and should therefore have very similar collision diameters if electronic effects dominate. Viscosity measurements [Lide, 2001] indicate that the collision diameters of these molecules are nearly identical (3.697 and 3.708 Å for N₂ and CO, respectively, a difference of 1 part in 300), whereas the molecular bond lengths are quite different (1.094 and 1.1282 Å, respectively, a difference 10 times larger) [Sutton, 1965]. CO is not symmetric; thus the distance between the carbon atom and the center of mass increases the apparent molecular size of CO to 1.2894 Å (making the difference nearly 50 times larger).

[23] The ratio of the diffusivities of CO and N₂ in O₂, $D_{CO,O_2}/D_{N_2,O_2}$, can be calculated from equation (8) using both viscosity-derived collision diameters and bond lengths. It is found that

$$D_{CO,O_2}/D_{N_2,O_2} (\text{viscosity}) = 0.997$$

$$D_{CO,O_2}/D_{N_2,O_2} (\text{bond lengths}) = 0.850$$

$$D_{CO,O_2}/D_{N_2,O_2} (\text{experimental}) = 0.999,$$

where the experimental value is taken from Massman [1998]. (The O₂ collision diameter used is 3.546 Å and the O₂ bond length 1.207 Å.) The viscosity-derived ratio is much closer to the experimental ratio than the bond-length-derived ratio indicating that it is the collision diameter and not explicitly the bond lengths and angles that are important in controlling molecular diffusion. Considering the similarity of the molecular diffusion constants for CO and N₂ and the large difference in bond lengths, it is unlikely that the slight differences in the molecular dimensions of the water isotopomers would lead to significant differences in the collision diameters or diffusion constants.

3.3. Atmospheric Implications

[24] The isotopic composition of evaporation is calculated according to

$$(\delta_E/1000 + 1) = \alpha_{eff}^*(\delta_L/1000 + 1), \quad (7)$$

where δ_E is the isotopic composition of the evaporation and δ_L is the isotopic composition of the water. The α_{eff}^* is as given in equation (5) and is dependent on temperature, relative humidity, $\alpha_{diffusion}^*$, and δ_a ($\delta_a \equiv$ the isotopic composition of the atmosphere with respect to the ocean). Isotope fractionation during evaporation in GCMs is typically implemented according to the formulation of

Merlivat and Jouzel [1979], which is based on M78 and has no role for the evaporation rate effect on surface temperature. In the work of Merlivat and Jouzel [1979] the formulation for $\alpha_{\text{diffusion}}^*$ is

$$\alpha_{\text{diffusion}}^* = \frac{[D_L/D_H]^n - 1}{[D_L/D_H]^n + \rho_T/\rho_M}, \quad (8)$$

where ρ_T and ρ_M are the turbulent and molecular resistances [Brutsaert, 1975a, 1975b], respectively, which depend on various geophysical parameters including horizontal wind speed at 10 m and air viscosity. The value of n is dependent on whether the water-atmosphere interface is smooth or rough. Explicit expressions to calculate ρ_T/ρ_M for both smooth and rough interfaces are given by Merlivat and Jouzel [1979], but they also show a simple relationship between $\alpha_{\text{diffusion}}^*$ and 10-m wind speed (in Merlivat and Jouzel [1979] $\alpha_{\text{diffusion}}^*$ is referred to as k). In our analysis above we have used an approximate form of equation (8), which is more appropriate to laboratory conditions, to describe the diffusion-controlled fractionation (see equation (5)).

[25] The difference in δ_E calculated using the surface-cooling model of evaporation described in this paper (henceforth referred to as the CHDC model) with $\Gamma_L = \Gamma_H$ instead of the M78 model is controlled by the variation in $\alpha_{\text{diffusion}}^*$, which depends explicitly on the values of D_H/D_L used. As an example, $\alpha_{\text{diffusion}}^*$ is calculated from equation (8) using D_H/D_L values from both the CHDC and the M78 models assuming a smooth interface with a 10-m wind speed of $U = 5$ m/s ($\rho_T/\rho_M = 2.01$): The isotope effects ($\epsilon_{\text{diffusion}}^* = 1000(1 - \alpha_{\text{diffusion}}^*)$) are $\epsilon_{\text{diffusion,CHDC}}^*(D/H) = 3.61\text{‰}$ and $\epsilon_{\text{diffusion,CHDC}}^*(^{18}\text{O}/^{16}\text{O}) = 6.98\text{‰}$; $\epsilon_{\text{diffusion,M78}}^*(D/H) = 5.51\text{‰}$ and $\epsilon_{\text{diffusion,M78}}^*(^{18}\text{O}/^{16}\text{O}) = 6.25\text{‰}$. It is interesting to note that $\epsilon_{\text{diffusion,CHDC}}^*(D/H)$ is smaller than $\epsilon_{\text{diffusion,M78}}^*(D/H)$, while $\epsilon_{\text{diffusion,CHDC}}^*(^{18}\text{O}/^{16}\text{O})$ is slightly larger than $\epsilon_{\text{diffusion,M78}}^*(^{18}\text{O}/^{16}\text{O})$. Continuing the example, the value of δ_E is determined from these values of $\alpha_{\text{diffusion}}^*$ over the range $0.6 \leq h < 0.8$ by substitution in equation (7).

[26] The specific values of δ_E that are obtained depend strongly on the values used for δ_a . However, it is found that the difference $\Delta_E(^{18}\text{O} \text{ or } D) = \delta_{E,\text{CHDC}} - \delta_{E,\text{M78}}$ or $\Delta_E(d) = d_{\text{CHDC}} - d_{\text{M78}}$ is nearly constant over a large range of δ_a . We use $\delta_a D = -86\text{‰}$ and $\delta_a ^{18}\text{O} = -12\text{‰}$ (which are reasonable values at low latitudes, where most evaporation occurs) such that $d_a = +10\text{‰}$. We estimate the extent of surface cooling in a given region by consideration of observed evaporation rates. In the subtropics where annual mean evaporation rates are approximately 1.5 m yr^{-1} [Peixoto and Oort, 1992] a surface cooling of 1.6°C is predicted from the results of Fang and Ward [1999]. This surface cooling is taken into account by calculating Δ_E at $T = 23.4^\circ\text{C}$ for the CHDC model, while for the M78 model $T = 25^\circ\text{C}$. It is found that $-1.1\text{‰} > \Delta_E(^{18}\text{O}) > -1.4\text{‰}$ and $-2.1\text{‰} > \Delta_E(D) > -5.6\text{‰}$ over the range 60–80% h . For the deuterium excess, $6.4\text{‰} > \Delta_E(d) > 5.4\text{‰}$ over the same range. Thus if the M78 diffusivity ratios are used to calculate k , d is underestimated by about 6‰, while both $\delta^{18}\text{O}$ and δD are overestimated relative to the CHDC model. This difference is sensitive to relative humidity because kinetic effects contribute to a greater extent to the total fractionation as humidity decreases (see equation (4)), as is

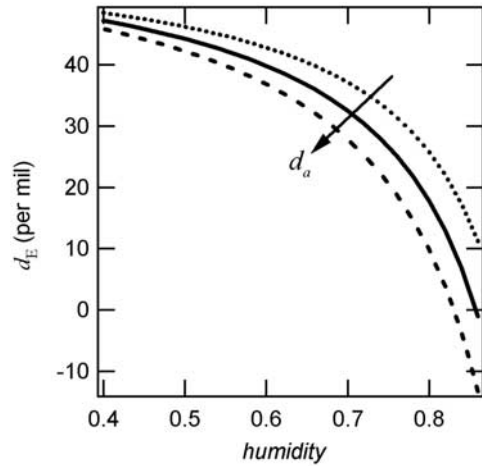


Figure 5. Deuterium excess values calculated for the net evaporate as a function of humidity with $T_{\text{surface}} = 25^\circ\text{C}$. The solid line corresponds to $\delta D_a = -86\text{‰}$, $\delta^{18}\text{O}_a = -12\text{‰}$, and $d_a = +10\text{‰}$. For the dashed line $\delta D_a = -84\text{‰}$ such that $d_a = +12\text{‰}$ and for the dotted line $\delta D_a = -88\text{‰}$ such that $d_a = +8\text{‰}$.

seen in the variation in the Δ_E values given above. Additionally, this humidity effect is evident in the absolute d values calculated for the above conditions, with d changing from $\sim 0\text{‰}$ at $h = 86\%$ to 47‰ at $h = 40\%$ for our model (Figure 5). This variation in d with humidity is independent of the values specified for δ_a so long as d_a is held constant. However, when d_a is increased (decreased) from $+10\text{‰}$ d decreases (increases) for a given value of h .

[27] Evaporative cooling of the ocean surface has been observed experimentally through comparison of radiometric measurements of the open ocean surface temperature, which are sensitive to the top $\sim 10 \mu\text{m}$ of the ocean surface, to simultaneous thermistor measurements of the bulk ocean [Wick et al., 1996; Donlon et al., 1999]. The extent of oceanic surface cooling has been shown to depend on wind speed, with coolings up to 0.6°C observed at low wind speeds ($< 5 \text{ m s}^{-1}$). The larger surface coolings observed by Fang and Ward [1999] may be explained by the static conditions, relative to the open ocean, of their laboratory experiments. It is important to note that as wind speed decreases, equilibrium fractionation decreases because surface cooling is less significant, whereas diffusive fractionation, as predicted by the Merlivat and Jouzel [1979] model, increases. If $\Delta T = 0.6^\circ\text{C}$ is instead used for the difference between the CHDC and M78 models, $0.3\text{‰} > \Delta_E(^{18}\text{O}) > -0.9\text{‰}$, $-0.9\text{‰} > \Delta_E(D) > -1.0\text{‰}$ and $7.2\text{‰} > \Delta_E(d) > 6.9\text{‰}$ over the range 60–80% h . Despite the decrease in the amount of surface cooling assumed compared to above, the deviation in the deuterium excess increases to about 7‰ between the CHDC and M78 models.

[28] Hoffmann et al. [1998], using the ECHAM3-T42 GCM, found the results for annual average deuterium excess values of Antarctic precipitation 2–5‰ lower than observations. We have shown that inclusion of more realistic diffusivity ratios and surface cooling due to evaporation forces d in the direction of this discrepancy for the initial evaporating vapor. Evidently, it is necessary to

completely explore the magnitude of this effect and how it affects d globally (particularly at high latitudes) through implementation into GCMs; however, the difference in $\Delta_E(d)$ predicted from this analysis is large and should be observable in GCMs in addition to the smaller differences in $\Delta_E(^{18}\text{O})$ and $\Delta_E(\text{D})$.

4. Conclusions

[29] The effects of diffusion-controlled fractionation during evaporation under nonequilibrium conditions have been investigated. When modeling water isotope fractionation it is necessary to consider the surface temperature rather than the bulk temperature of the evaporating liquid, as it is this temperature that determines the equilibrium fractionation factors to be used. Once surface cooling is properly accounted for in laboratory measurements we have shown that the ratio of molecular diffusivities of isotopic water molecules is well represented by the classical kinetic theory of gases, i.e., there is no observable isotope dependence in effective molecular collision diameter as suggested by M78. We suggest that these isotope diffusivity ratios ($D_{18\text{o}}/D_{16\text{o}} = 0.9691$ and $D_{\text{D}}/D_{\text{H}} = 0.9839$) should be used when modeling water isotope fractionation.

[30] These results have an important consequence for the inclusion of water isotopes in GCMs and other simple models as the parameterization of isotope fractionation during evaporation depends on both the molecular diffusivity ratios and the specified surface temperature. Use of the M78 diffusivity ratios in evaporation models yields deuterium excess values that are too small compared with the CHDC model presented here in which the kinetic theory diffusivity ratios are used and surface cooling is explicitly accounted for. In addition, molecular diffusion is believed to play a major role in fractionating isotopes during the formation of ice crystals in clouds at $T < -20^\circ\text{C}$ [Jouzel and Merlivat, 1984]. The change in diffusivity ratios we advocate will have significant impact on the isotopic composition of high-latitude precipitation where cloud temperatures are below 20°C .

[31] When modeling water isotope fractionation it is necessary to consider the surface temperature rather than the bulk temperature of the evaporating liquid, as it is this temperature that determines the equilibrium fractionation factors to be used. Experimentally it may prove difficult to measure the amount of cooling at the surface of the ocean or a lake, although use of radiometric measurements of surface temperature combined with in situ bulk temperature measurements show promise in this regard. However, in order to consider surface cooling on a global scale, we suggest that observed or modeled evaporation rates can be used to infer the surface cooling using the laboratory measurements of Fang and Ward [1999]. This would provide a method to account for surface cooling in GCMs that include water isotopes.

Appendix A: Steady State Evaporation Model

[32] Evaporation is modeled assuming a turbulent boundary layer separates the liquid surface from the well-mixed free atmosphere (see Figure A1). If the water vapor profile in this boundary layer is at steady state, it is necessary that

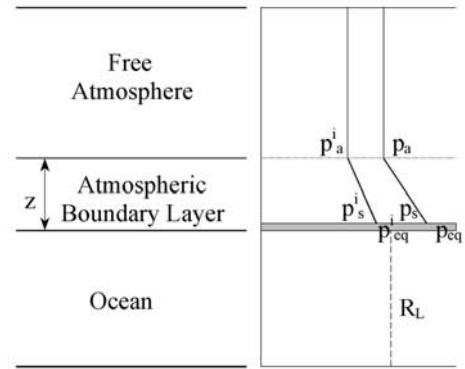


Figure A1. Model of evaporation. The vapor pressure of H_2O is p and the vapor pressure of H_2^{18}O or HDO is p^i . The subscript a indicates conditions of the free atmosphere, s indicates the actual conditions of the atmosphere at the ocean-boundary layer interface and eq indicates conditions of the atmosphere in equilibrium with the ocean at the temperature of the ocean-boundary layer interface.

the fluxes of all molecular species across the boundary layer-free atmosphere interface are equal to the fluxes across the liquid-boundary layer interface. Isotopic fractionation occurs during transport across the liquid-air interface and during transport through the boundary layer.

[33] The net flux of water through the boundary layer-free atmosphere interface is

$$E = K \left[\frac{p_s - p_a}{z} \right], \quad (\text{A1})$$

where E is the evaporation rate, p_s is vapor pressure of water immediately above the liquid surface, p_a is the water vapor pressure in the free atmosphere, z is the boundary layer height, and K is an effective diffusivity that combines the effects of molecular and turbulent diffusion.

[34] The isotopic ratio of water transported into the free atmosphere, R_e , is defined as the ratio of equation (A1) for the isotopic species (either H_2^{18}O or HDO) to that for H_2O such that

$$R_e = \frac{E^i}{E} = \frac{K^i}{K} \left[\frac{p_s^i - p_a^i}{p_s - p_a} \right]. \quad (\text{A2})$$

[35] At the liquid-boundary layer interface the net flux of water is described by

$$E = \gamma(p_{eq} - p_s), \quad (\text{A3})$$

where

$$\gamma = \chi(2\pi mkT)^{-1/2} \quad (\text{A4})$$

and p_{eq} is the saturation vapor pressure of H_2O at the liquid surface, m is the molecular mass of the H_2O , and k is the Boltzmann constant. The evaporation/condensation coefficient χ for water defined as the ratio of the number of gaseous molecules that condense on the liquid surface to the total number of gaseous molecules that strike the surface.

When relative humidity at the liquid surface is 100% $p_{\text{eq}} = p_s$ and the net evaporation rate is zero.

[36] Since at steady state the fluxes through the liquid-air interface (equation (A4)) and the boundary layer-free atmosphere interface (equation (A1)) are equal it is found that

$$K \left[\frac{p_s - p_a}{z} \right] = \gamma (p_{\text{eq}} - p_s). \quad (\text{A5})$$

[37] By solving equation (A5) and its isotopic analogue for p_s and p_s^i respectively, and substituting into equation (A2) we have an expression for the isotopic ratios in evaporation that is dependent on only the conditions of the free atmosphere and of the bulk liquid. It is not necessary to know the conditions at the surface.

$$R_e = \frac{K^i}{K} \left[\frac{p_{\text{eq}}^i + \frac{K^i}{\gamma^i z} p_a^i}{1 + \frac{K^i}{\gamma^i z}} - p_a^i \right] \left[\frac{p_{\text{eq}} + \frac{K}{\gamma z} p_a}{1 + \frac{K}{\gamma z}} - p_a \right]^{-1}. \quad (\text{A6})$$

[38] This equation is greatly simplified by writing it in terms of isotopic ratios (R_x) and humidities relative to the saturation vapor at conditions of the ocean surface (h_x). This is done by multiplying the numerator and denominator of equation (A6) by $1/p_{\text{eq}}$ and using the following substitution.

$$\frac{p_x^i}{p_{\text{eq}}} = \frac{p_x^i p_x}{p_x p_{\text{eq}}} = R_x h_x, \quad (\text{A7})$$

where $x = \text{eq}, s,$ or a . If $x = \text{eq}, h_x = 1$. The result is a useful expression for the isotopic ratio of evaporation:

$$R_e = \frac{K^i}{K} \left[\frac{1 + K/\gamma z}{1 + K^i/\gamma^i z} \right] \left[\frac{R_{\text{eq}} - h_a R_a}{1 - h_a} \right]. \quad (\text{A8})$$

[39] We define an effective fractionation factor as the ratio of the isotopic ratio in evaporation to the isotopic ratio of the liquid ($\alpha_{\text{eff}} = R_e/R_L$).

$$\alpha_{\text{eff}}^* = \frac{R_e}{R_L} = \alpha_{\text{diffusion}}^* \left[\frac{\alpha_{\text{eqm}}^* - h_a \frac{R_a}{R_L}}{1 - h_a} \right], \quad (\text{A9})$$

where

$$\alpha_{\text{diffusion}}^* = \frac{K^i}{K} \left[\frac{1 + K/\gamma z}{1 + K^i/\gamma^i z} \right], \quad (\text{A10})$$

and α_{eqm}^* is the equilibrium fractionation factor (R_{eq}/R_L). From equation (A10) we see that the diffusion-controlled fractionation factor, $\alpha_{\text{diffusion}}^*$, depends on the size of the boundary layer, diffusivities, and γ , which depends on temperature, molecular masses, and evaporation/condensation coefficients. However, equation (A10) can be approximated as $\alpha_{\text{diffusion}}^* = K^i/K$ because $\gamma = O(10^{22} \text{ s m}^{-1} \text{ kg}^{-1})$, whereas z will range from cm to m and K from 10^{-5} to $1 \text{ m}^2 \text{ s}^{-1}$. Thus the term in brackets is nearly unity.

[40] **Acknowledgments.** This material is based on work supported by the National Science Foundation Atmospheric Chemistry Program under

grant 0138669. Support was also provided by the Chemical Sciences, Geosciences, and Biosciences program, DOE Office of Science through contract DE-AC03-76SF00098. C.D.C. is supported by the Department of Defense National Defense Science and Engineering Fellowship, the American Meteorological Society/Department of Energy Atmospheric Radiation Measurement Program Graduate Fellowship, and the UC Berkeley Atmospheric Sciences Center.

References

- Armengaud, A., R. D. Koster, J. Jouzel, and P. Ciais, Deuterium excess in Greenland snow: Analysis with simple and complex models, *J. Geophys. Res.*, 103(D8), 8947–8953, 1998.
- Bender, M., T. Sowers, and L. Labeyrie, The Dole effect and its variations during the last 13,000 years as measured in the Vostok ice core, *Global Biogeochem. Cycles*, 8(3), 363–376, 1994.
- Bigeleisen, J., Statistical mechanics of isotope effects on the thermodynamic properties of condensed systems, *J. Chem. Phys.*, 34(5), 1485–1493, 1961.
- Bottinga, Y., and H. Craig, Oxygen isotope fractionation between CO_2 and water and the isotopic composition of marine atmospheric CO_2 , *Earth Planet Sci. Lett.*, 5, 285–295, 1969.
- Brutsaert, W., The roughness length for water vapor, sensible heat, and other scalars, *J. Atmos. Sci.*, 32, 2028–2031, 1975a.
- Brutsaert, W., A theory for local evaporation (or heat transfer) from rough and smooth surfaces at ground level, *Water Resour. Res.*, 11(4), 543–550, 1975b.
- Craig, H., and L. I. Gordon, *Stable Isotope in Oceanographic Studies and Paleotemperatures*, 122 pp., V. Lischi e Figli, Pisa, 1965.
- Craig, H., L. I. Gordon, and Y. Horibe, Isotopic exchange effects in the evaporation of water, *J. Geophys. Res.*, 68(17), 5079–5087, 1963.
- Cuffey, K. M., R. B. Alley, P. M. Grootes, J. M. Bolzan, and S. Anandakrishnan, Calibration of the Delta-O-18 isotopic paleothermometer for central greenland, using borehole temperatures, *J. Glaciol.*, 40(135), 341–349, 1994.
- Dansgaard, W., Stable isotopes in precipitation, *Tellus*, 16(4), 436–468, 1964.
- Donlon, C. J., T. J. Nightingale, T. Sheasby, J. Turner, I. S. Robinson, and W. J. Emery, Implications of the oceanic thermal skin temperature deviation at high wind speed, *Geophys. Res. Lett.*, 26(16), 2505–2508, 1999.
- Donnelly, T., S. Waldron, A. Tait, J. Dougans, and S. Bearhop, Hydrogen isotope analysis of natural abundance and deuterium-enriched waters by reduction over chromium on-line to a dynamic dual inlet isotope-ratio mass spectrometer, *Rapid Commun. Mass Spectrom.*, 15(15), 1297–1303, 2001.
- Fang, G., and C. A. Ward, Temperature measured close to the interface of an evaporating liquid, *Phys. Rev. E*, 59(1), 417–428, 1999.
- Farquhar, G. D., J. Lloyd, J. A. Taylor, L. B. Flanagan, J. P. Syvertsen, K. T. Hubick, S. C. Wong, and J. R. Ehleringer, Vegetation effects on the isotope composition of oxygen in atmospheric CO_2 , *Nature*, 365(6444), 368, 1993.
- Hendricks, M. B., A one-dimensional model of hydrogen and oxygen isotopic ratios in the global hydrologic cycle, Ph.D. Dissertation thesis, Univ. of Calif., Berkeley, 1999.
- Hendricks, M. B., D. J. DePaolo, and R. C. Cohen, Space and time variation of $\delta^{18}\text{O}$ and δD in precipitation: Can paleotemperature be estimated from ice cores?, *Global Biogeochem. Cycles*, 14(3), 851–861, 2000.
- Hirschfelder, J. O., *Molecular Theory of Gases and Liquids*, 1219 pp., John Wiley, Hoboken, N.J., 1954.
- Hoffmann, G., M. Werner, and M. Heimann, Water isotope module of the ECHAM atmospheric general circulation model: A study on timescales from days to several years, *J. Geophys. Res.*, 103(D18), 16,871–16,896, 1998.
- Horita, J., and D. J. Wesolowski, Liquid-vapor fractionation of oxygen and hydrogen isotopes of water from the freezing to the critical temperature, *Geochim. Cosmochim. Acta*, 58(16), 3425–3437, 1994.
- Jouzel, J., and L. Merlivat, Deuterium and oxygen 18 in precipitation: Modeling of the isotopic effects during snow formation, *J. Geophys. Res.*, 89(D7), 11,749–11,757, 1984.
- Jouzel, J., G. Russell, R. Suozzo, R. Koster, and J. W. C. White, Simulations of the HDO and H₂O-18 atmospheric cycles using the NASA/GISS general circulation model: The seasonal cycle for present day conditions, *J. Geophys. Res.*, 92(D12), 14,739–14,760, 1987.
- Jouzel, J., et al., Validity of the temperature reconstruction from water isotopes in ice cores, *J. Geophys. Res.*, 102(C12), 26,471–26,487, 1997.
- Jouzel, J., G. Hoffmann, R. D. Koster, and V. Masson, Water isotopes in precipitation: Data/model comparison for present-day and past climates, *Quat. Sci. Rev.*, 19(1–5), 363–379, 2000.
- Kavanaugh, J. L., and K. M. Cuffey, Space and time variation of $\delta^{18}\text{O}$ and δD in Antarctic precipitation, revisited, *Global Biogeochem. Cycles*, 17(1), 1017, doi:10.1029/2002GB001910, 2003.

- Lide, D. R., *CRC Handbook of Chemistry and Physics*, CRC Press, Boca Raton, Fla., 2001.
- Massman, W. J., A review of the molecular diffusivities of H₂O, CO₂, CH₄, CO, O₃, SO₂, NH₃, N₂O, NO, and NO₂ in air, O₂ and N₂ near STP, *Atmos. Environ.*, *32*(6), 1111–1127, 1998.
- Merlivat, L., Molecular diffusivities of H₂¹⁶O, HD¹⁶O and H₂¹⁸O in gases, *J. Phys. Chem.*, *69*(6), 2864–2871, 1978.
- Merlivat, L., and M. Coantic, Study of mass transfer at the air-water interface by an isotopic method, *J. Geophys. Res.*, *80*(24), 3455–3464, 1975.
- Merlivat, L., and J. Jouzel, Global climatic interpretation of the deuterium-oxygen 18 relationship for precipitation, *J. Geophys. Res.*, *84*(C8), 5029–5033, 1979.
- Peixoto, J. P., and A. H. Oort, *Physics of Climate*, vol. 39, 520 pp., Am. Inst. of Phys., New York, 1992.
- Petit, J. R., et al., Climate and atmospheric history of the past 420,000 years from the Vostok ice core, Antarctica, *Nature*, *399*(6735), 429–436, 1999.
- Stewart, M. K., Stable isotope fractionation due to evaporation and isotopic exchange of falling waterdrops: Applications to atmospheric processes and evaporation of lakes, *J. Geophys. Res.*, *80*(9), 1133–1146, 1975.
- Sutton, L. E., *Tables of Interatomic Distances and Configuration in Molecules and Ions, Supplement, 1956–1959*, vol. 1, Chem. Soc., London, 1965.
- Vimeux, F., V. Masson, G. Delaygue, J. Jouzel, J. R. Petit, and M. Stievenard, A 420,000 year deuterium excess record from East Antarctica: Information on past changes in the origin of precipitation at Vostok, *J. Geophys. Res.*, *106*(D23), 31,863–31,873, 2001.
- von Caemmerer, S., and G. D. Farquhar, Some relationships between the biochemistry of photosynthesis and the gas exchange of leaves, *Planta*, *153*, 376–387, 1981.
- Ward, C. A., and D. Stanga, Interfacial conditions during evaporation or condensation of water, *Phys. Rev. E.*, *64*(5), 051509, U347–U354, 2001.
- Werner, M., M. Heimann, and G. Hoffmann, Stable water isotopes in Greenland ice cores: ECHAM 4 model simulations versus field measurements, in *International Symposium on Isotopes Techniques in the Study of Past and Current Environmental Changes in the Hydrosphere and the Atmosphere*, pp. 603–612, Int. At. Energy Agency, Vienna, 1998.
- Wexler, A., Vapor pressure formulation for water in the range 0 to 100 deg C: A revision, *J. Res. Natl. Bur. Stand., U.S., Sect. A*, *80*(5 and 6), 1976.
- White, J. W. C., L. K. Barlow, D. Fisher, P. Grootes, J. Jouzel, S. J. Johnsen, M. Stuiver, and H. Clausen, The climate signal in the stable isotopes of snow from Summit, Greenland: Results of comparisons with modern climate observations, *J. Geophys. Res.*, *102*(C12), 26,425–26,439, 1997.
- Wick, G. A., W. J. Emery, L. H. Kantha, and P. Schlusser, The behavior of the bulk-skin sea surface temperature difference under varying wind speed and heat flux, *J. Phys. Oceanogr.*, *26*(10), 1969–1988, 1996.

C. D. Cappa and R. C. Cohen, Department of Chemistry, University of California, B64A Hildebrand Hall, Berkeley, CA 94720-1460, USA. (cappa@uclink.berkeley.edu; cohen@cchem.berkeley.edu)

D. J. DePaolo, Department of Earth and Planetary Sciences, University of California, Berkeley, CA 94720-4767, USA. (depaolo@eps.berkeley.edu)

M. B. Hendricks, Department of Geosciences, Princeton University, Princeton, NJ 08544, USA. (mhendric@princeton.edu)